Ammonia Synthesis Hot Paper

International Edition: DOI: 10.1002/anie.201703695
German Edition: DOI: 10.1002/ange.201703695

# The Formation of Surface Lithium–Iron Ternary Hydride and its Function on Catalytic Ammonia Synthesis at Low Temperatures

*Peikun Wang[+], Hua Xie[+], Jianping Guo, Zhi Zhao, Xiangtao Kong, Wenbo Gao, Fei Chang, Teng He, Guotao Wu, Mingshu Chen, Ling Jiang,* and Ping Chen**

***Abstract:*** *Lithium hydride (LiH) has a strong effect on iron leading to an approximately 3 orders of magnitude increase in catalytic ammonia synthesis. The existence of lithium–iron ternary hydride species at the surface/interface of the catalyst were identified and characterized for the first time by gas-phase optical spectroscopy coupled with mass spectrometry and quantum chemical calculations. The ternary hydride species may serve as centers that readily activate and hydrogenate dinitrogen, forming Fe-($NH_2$)-Li and $LiNH_2$ moieties—possibly through a redox reaction of dinitrogen and hydridic hydrogen (LiH) that is mediated by iron—showing distinct differences from ammonia formation mediated by conventional iron or ruthenium-based catalysts. Hydrogen-associated activation and conversion of dinitrogen are discussed.*

Ammonia is one of the most important synthetic chemicals for the sustainable growth of human society because it is the nitrogen (N) source of manmade fertilizer and a promising energy carrier in the upcoming renewable energy era.[1] The activation and transformation of dinitrogen ($N_2$) under mild conditions is thus one of the grand challenges in chemistry and has been pursued actively for a century.[1a,2] Advanced surface-science investigations and theoretical calculations have demonstrated that the dissociative activation of $N_2$ on active sites made of multiple transition metal atoms (for example, the C7 site of Fe catalysts) is the slow elementary step.[3] Alkali metals (except Li), in their oxidative form, are electronic promoters that enhance the catalytic activity of Fe through electron donation or electrostatic effect.[2e,4] Since both the activation energies and adsorption energies of reacting adspecies are dominated by the electronic properties of transition metals and obey the scaling relations, efficient ammonia synthesis at low temperatures can hardly be achieved.[2e,5]

Recently, ammonia synthesis at low temperatures (such as, 150 °C) was recorded upon employing TM-LiH (transition metal (TM) = Cr, Mn, Fe, Co) composites as catalysts.[6] Kinetic analyses show that these catalysts have smaller apparent activation energies (45–65 kJ mol$^{-1}$) and lower reaction orders of $N_2$ (ca. 0.5), implying that the rate-determining step is unlikely to be the dissociation of $N_2$. To determine the mechanistic foundation of this new TM-LiH catalytic system for the multielectron and multihydrogen process, a number of imperative questions should be addressed: 1) the nature of the active site; 2) the manner in which $N_2$ is activated; 3) the site of $NH_3$ formation, and so forth. These issues are crucial for a molecular-level understanding of ammonia synthesis over the TM-LiH composite catalyst and directive for the design and optimization of catalytic material, but difficult to completely elucidate solely with conventional condensed-phase characterization techniques. Gas-phase clusters, bombarded from the surface of a catalyst and efficiently cooled by supersonic expansion of pulsed carrier gas, contains compositional and structural information of the surface and may represent the most active or least coordinated site on the surface.[7] The reaction between those clusters and gaseous reactants can thus provide structural and energetic information for mechanistic understanding of a catalytic process.[7,8] Combined with the condensed-phase approaches, herein, the gas-phase optical spectroscopy coupled with mass spectrometry (GOS-MS) supplemented with density functional theory (DFT) calculations was employed to characterize the active site, reactive surface species, and intermediates of the Fe-LiH catalyst, and to provide detailed insights into the microscopic mechanism of the activation and transformation of $N_2$ on that catalyst surface.

We first tested the effect of LiH content on the catalytic performance of the Fe-LiH composite (Figure 1). The activity of neat polycrystalline Fe is negligible, which is about 2 to 3 orders of magnitude lower than that of the Fe-*x*LiH ($x = 1$–693) catalysts. The Fe-LiH, Fe-3LiH, Fe-5LiH, and Fe-10LiH catalysts show similar ammonia synthesis rates in terms of the

[*] P. K. Wang,[+] Dr. H. Xie,[+] Dr. J. P. Guo, Z. Zhao, X. T. Kong, W. B. Gao, F. Chang, Dr. T. He, Prof. G. T. Wu, Prof. Dr. L. Jiang, Prof. Dr. P. Chen
Dalian Institute of Chemical Physics, Chinese Academy of Sciences
Dalian 116023 (China)
E-mail: ljiang@dicp.ac.cn
pchen@dicp.ac.cn
P. K. Wang,[+] X. T. Kong, W. B. Gao, F. Chang
University of Chinese Academy of Sciences
Beijing 100049 (China)
Dr. H. Xie,[+] Z. Zhao, X. T. Kong, Prof. Dr. L. Jiang
State Key Laboratory of Molecular Reaction Dynamics, Dalian Institute of Chemical Physics, Chinese Academy of Sciences
Dalian 116023 (China)
Dr. J. P. Guo, Prof. Dr. L. Jiang, Prof. Dr. P. Chen
Collaborative Innovation Center of Chemistry for Energy Materials
Dalian Institute of Chemical Physics, Chinese Academy of Sciences
Dalian 116023 (China)
Prof. Dr. M. S. Chen
State Key Laboratory of Physical Chemistry of Solid Surfaces
Department of Chemistry, Xiamen University
Xiamen 361005 (China)
[+] These authors contributed equally to this work.
Supporting information and the ORCID identification number(s) for the author(s) of this article can be found under: https://doi.org/10.1002/anie.201703695.

  

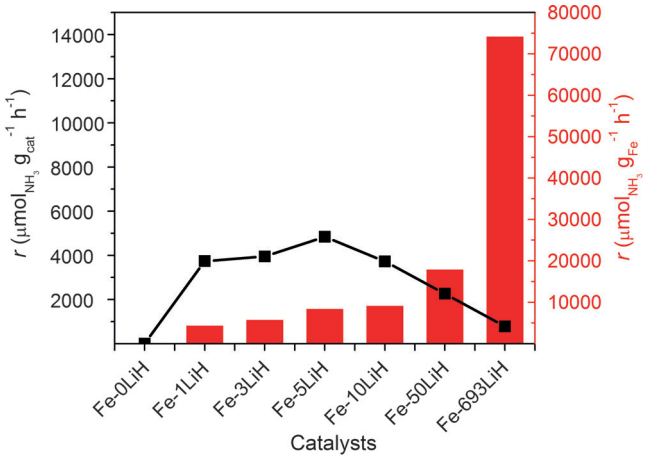


***Figure 1.*** Ammonia synthesis performances of Fe-*x*LiH catalysts at 300 °C. Reaction conditions: catalyst (30 mg), syngas ($N_2 + 3\,H_2$; 10 bar), flow rate (30 mL min$^{-1}$).

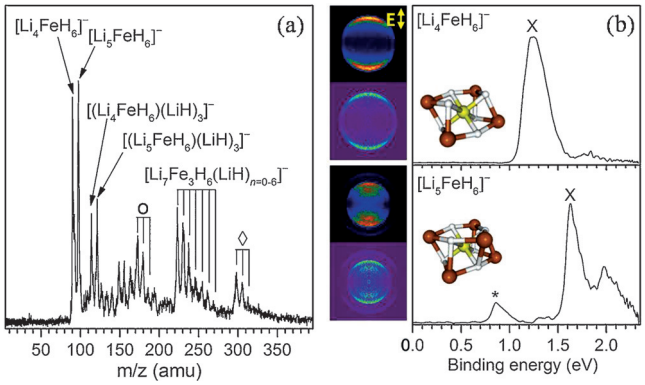


***Figure 2.*** a) Mass spectrum of the species produced by pulsed laser vaporization of the Fe-LiH target in the presence of a helium carrier gas (mass peaks: $[Li_7Fe_2H_{11}(LiH)_{n=0-2}]^-$ (○), $[Li_9Fe_3H_{11}(LiH)_{n=0-2}]^-$ (◇)); b) Photoelectron images and spectra of $[Li_4FeH_6]^-$ and $[Li_5FeH_6]^-$ at 532 nm (2.331 eV). The raw image (upper) and the reconstructed image (lower) for each cluster; the central panel corresponds to the clusters after inverse Abel transformation. The double arrow indicates the direction of the laser polarization. The peak (*) denotes the excited state of the anion.

weight of catalyst, among which the Fe-5LiH performs slightly better. However, even by reducing Fe content by a factor of approximately 58 (that is, from Fe-5LiH to Fe-693LiH), the ammonia formation rate drops only by a factor of about six. Therefore, we calculate the $NH_3$ formation rate with respect to the amount of Fe. As shown in Figure 1, there is a monotonic but not proportional increase in activity with a decrease of Fe content, where Fe-693LiH has an activity of approximately $7.4 \times 10^4$ $\mu mol_{NH_3}\,g_{Fe}^{-1}\,h^{-1}$. Such a monotonic increase in activity with respect to Fe amount in Fe-*x*LiH may reflect the importance of contact or interface between LiH and Fe particles in catalyzing ammonia formation; that is, a lower iron loading would result in smaller Fe particles that would have higher surface area to contact with neighboring LiH. As a matter of fact, the Fe-693LiH samples before and after testing have an average Fe particle size (ca. 1.70 nm), which is obviously smaller than that of Fe-10LiH (> 10 nm; Supporting Information, Figures S1 and S2). The value of turnover frequency (TOF) of the Fe-693LiH at 300 °C calculated from the dispersion of Fe[9] is $2.16 \times 10^{-3}$ $s^{-1}$, which is comparable to that of the highly active Cs-promoted Ru/MgO catalysts[10] and also indicates a remarkable synergy between LiH and Fe. Therefore, we prepared MgO supported Fe-5LiH catalyst (Fe content is 10 wt % of MgO) to achieve better Fe dispersion and to reduce Fe and LiH contents. To our delight, with an approximately 85 % decrease in Fe and LiH contents the supported catalyst outperforms the neat Fe-5LiH composite by 30 % at 300 °C, and its $NH_3$ formation rate is significantly higher than that for Cs-Ru/MgO (Supporting Information, Figure S3), especially at low temperatures.

Powder X-ray diffraction (PXRD) characterizations of the Fe-5LiH samples collected in situ under a flow of hydrogen show the presences of Fe and LiH bulk phases. However, in the temperature-programmed decomposition (TPD) measurement, a hydrogen signal was clearly observed in the temperature range of 100 to 350 °C for the hydrogenated Fe-5LiH, but not for neat LiH (Supporting Information, Figure S4). The presences of Li–Fe ternary hydride species was confirmed by gas-phase photoelectron velocity-map imaging spectroscopic experiments and quantum chemical calculations. As depicted in Figure 2 a, the most intense peaks in the mass spectrum of clusters bombarded from the Fe-LiH sample are observed at $m/z = 90$ and 97 amu, which are assigned to the $[Li_4FeH_6]^-$ and $[Li_5FeH_6]^-$ clusters, respectively. The photoelectron spectrum of each cluster has one broad ground band (Figure 2 b). The vertical detachment energies (VDEs) of $[Li_4FeH_6]^-$ and $[Li_5FeH_6]^-$ are estimated from their X band maxima to be 1.22 and 1.63 eV, respectively. The $[Li_4FeH_6]^-$ cluster is identified to have a $C_2$ structure with a $^2B$ ground state. The calculated VDE of $[Li_4FeH_6]^-$ is 1.03 eV, which is consistent with the experimental value of 1.22 eV. Six hydrogen atoms are bound to the Fe atom, which is isostructural to $Li_4RuH_6$ and $Li_4OsH_6$.[11] Analogously, the $[Li_5FeH_6]^-$ complex has a $C_s$ structure with a $^3A''$ ground state (Figure 2 b). The fifth lithium atom is coordinated to the open sites of three hydrogen atoms. The VDE value is calculated to be 1.82 eV, reproducing the experiment well.

It was reported that the reaction enthalpy change of Equation 1 is about $-54$ kJ mol$^{-1}$ $H_2$, implying that the formation of $Li_4FeH_6$ is thermodynamically allowed, albeit kinetically difficult.[12]

$$Fe + 4\,LiH + H_2 \rightarrow Li_4FeH_6 \qquad (1)$$

We suppose that $[Li_4FeH_6]^-$ and $[Li_5FeH_6]^-$ detected by GOS-MS stem from the surface $Li_4FeH_6$ species because the coordinatively unsaturated nature of the surface Fe and LiH would be in favor of its formation.

$N_2$ absorptions on the Fe-5LiH and neat LiH samples were characterized by thermogravimetry (TG; Supporting Information, Figure S6). Observable weight gain starts at

  

about 150 °C for the fresh sample. Upon heating the sample in $N_2$ to 400 °C, approximately 30 wt % $N_2$ was absorbed by the sample. Fourier transform infrared spectroscopy (FTIR) and PXRD characterizations of the post-TG sample indicate the presence of $Li_2NH$ (Supporting Information, Figure S7). Because the nitridation of Fe under such conditions can be negligible, an approximately 30 wt % weight gain would mainly correspond to the conversion of 82 % LiH to $Li_2NH$. However, no observable reaction between LiH and $N_2$ takes place below 350 °C, which manifests the importance of Fe in the activation and supply of $N_2$ to LiH. Perceptibly, the interface of LiH and Fe, where the Li-Fe-H species may exist, could be the arena where the $N_2$ activation, transfer, and conversion take place, which is supported at least partially by the intriguing phenomenon; that is, the differentiated $N_2$ uptake feature and the $H_2$ desorption curve of the Fe-5LiH (Supporting Information, Figures S6 and S4a) has a similar temperature range and peak temperature. Such a coincidence may indicate that the ternary hydride species may be the site for $N_2$ activation, transfer, and conversion. The Fe-coordinated hydrogen in the hydride complexes exchanges with $N_2$ when $N_2$ approaches the transition-metal center, which resembles the phenomenon observed in homogeneous $N_2$ fixation.[13]

The interaction between $N_2$ and the Li-Fe-H species was further characterized by GOS-MS-DFT. No species was detected in the LiH + $N_2$ reaction (Figure 3a), implying that neat LiH is not reactive toward $N_2$, and the $[Li_xH_y]^-$ clusters are not readily formed in the $N_2$ environment. The Fe + $N_2$ reaction produces the $[FeN(N_2)_{1-6}]^-$ and $[NFeN(N_2)_{0-4}]^-$ clusters, showing the occurrence of the dissociative activation of $N_2$ and chemisorption of $N_2$ on neat Fe (Figure 3b). $[FeO(N_2)_{2-5}]^-$ and $[OFeO(N_2)_{2-6}]^-$ are also present, which is due to the fact that the iron oxides are readily formed and difficult to remove completely. Obviously, oxidized Fe is unable to dissociate $N_2$. By comparison, the $\{FeNH_2{\cdot}[(LiNH_2)_2H_2]_{0-1}\}^-$, $\{FeNH_2{\cdot}Li{\cdot}(LiNH_2)_2H_2]_{0-1}\}^-$, and $\{Li_5FeH_6{\cdot}[(LiNH_2)_2H_2]_{0-4}\}^-$ clusters were clearly detected in the Fe-5LiH + $N_2$ reaction (Figure 3c). The very important information about the reaction of $N_2$ and Li-Fe-H species disclosed by this gas-cluster reaction is summarized as follows: 1) the N≡N bond can be broken easily and the activated N can be hydrogenated to -$NH_2$ by hydridic H in the Li-Fe-H species; 2) some N bond with Li to form the $LiNH_2$ moiety exclusively, and some bridge with both Fe and Li, which indicates the transfer of activated N from Fe to Li; 3) no chemisorbed $N_2$ can be found in the Li-containing clusters; 4) the transfer of hydridic H (in $Li_4FeH_6$ and $Li_5FeH_6$) to protonic H (in $NH_2$) may stop at atomic H, which is attributed to the presence of the Fe-H moiety. $[NFeN(N_2)_{0-4}]^-$ clusters also present in the Fe-5LiH + $N_2$ reaction (but with weakened intensities as compared to those in the Fe + $N_2$ reaction), show that not all Fe in Fe-5LiH is in contact with LiH. The contrast between neat Fe and Fe-LiH reactions with $N_2$ clearly reveals the unique function of the Li–Fe ternary hydride species.

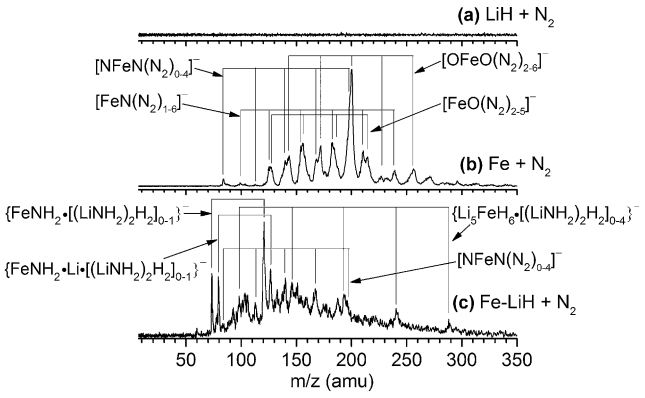


***Figure 3.*** Mass spectra of the species produced by pulsed laser vaporization of a) LiH, b) Fe, c) and Fe-LiH targets in the presence of a nitrogen carrier gas.

Among the series of products generated from the LiH-Fe + $N_2$ reactions, the representative $[FeNH_2]^-$ cluster was selected to for measurement using photoelectron spectroscopy (Supporting Information, Figure S8). The VDE of $[FeNH_2]^-$ is determined to be 2.03 eV. The $[FeNH_2]^-$ cluster is characterized to have a $C_s$ structure with a $^5A'$ ground state. The calculated VDE of $[FeNH_2]^-$ is 2.17 eV, which agrees with the experimental value. The representative reactions for the formation of the clusters shown in Figure 3c were investigated. Optimized structures of the main species are shown in Figure S9 (Supporting Information) and the calculated reaction energies are listed in Table S1 (Supporting Information). In the $[FeNH_2]^-$ cluster, the $NH_2$ subunit is formed and the distance and fuzzy bond order of Fe–N bond were calculated to be 1.914 Å and 1.584, respectively. The addition of an Li atom to the $[FeNH_2]^-$ cluster results in an exothermicity of $-150.5\ kJ\,mol^{-1}$ (Supporting Information, Table S1, reaction (1)), showing that the formation of $[FeNH_2{\cdot}Li]^-$ is thermodynamically favored. In the $[FeNH_2{\cdot}Li]^-$ cluster, the Li atom is bonded to the N atom, in which the Li–N bond distance is 1.956 Å (Supporting Information, Figure S9). Similarly, reactions (2)–(4) (Supporting Information) proceed exothermically by $-243.5$, $-332.0$, and $-227.1\ kJ\,mol^{-1}$, respectively. The Li–N bonds are further weakened in the larger clusters, such as $\{FeNH_2{\cdot}[(LiNH_2)_2H_2]\}^-$, $\{FeNH_2{\cdot}Li{\cdot}(LiNH_2)_2H_2]\}^-$, and $\{Li_5FeH_6{\cdot}[(LiNH_2)_2H_2]\}^-$. This is also manifested by the decrease of fuzzy bond order with an increase of cluster size. These stable gas-phase $\{FeNH_2{\cdot}[(LiNH_2)_2H_2]_{0-1}\}^-$, $\{FeNH_2{\cdot}Li{\cdot}(LiNH_2)_2H_2]_{0-1}\}^-$, and $\{Li_5FeH_6{\cdot}[(LiNH_2)_2H_2]_{0-4}\}^-$ clusters may correlate with the active intermediates formed on the Fe-5LiH surface upon $N_2$ interaction, and may further convert to Li-Fe-H and $LiNH_2$ through the exchange of -$NH_2$ with H of a neighboring LiH, or to Li-Fe-H and $NH_3$ through direct hydrogenation by molecular $H_2$.

As indicated by the GOS-MS and TPD analyses shown in the present work, the Li–Fe ternary hydride species (such as $Li_4FeH_6$) are thermally stable under pressurized hydrogen and present at the surface of the Fe-LiH sample as nicely supported by the predominated $[Li_4FeH_6]^-$ and $[Li_5FeH_6]^-$ clusters bombarded from the surface (Figure 2; Supporting Information, Figure S4a). Under the ammonia synthesis condition (7.5 bar hydrogen pressure and relatively lower temperatures), the aforementioned ternary hydride species

  

may have a certain concentration in the region where catalysis takes place. Consequently, the activation of $N_2$ on the Li-Fe-H center manifests the unique functions of ternary hydrides that highlight 1) the active site is no longer composed of multiple Fe atoms (that is, the C7 site of conventional Fe-based catalysts) but rather comprises a single Fe center surrounded by H and Li; 2) $N_2$ can be activated easily and partially hydrogenated to -$NH_x$ (Figure 3c; Supporting Information, Figures S6 and S7); 3) the activated N can be relocated to Li to be more stable; 4) the transformation of hydridic H (in Li-Fe-H) to protonic H (-$NH_2$) may pass through a Fe–H intermediate. If such functions can be linked to the surface catalytic phenomena of the Fe-LiH system, a better understanding on the superior low-temperature catalytic performance of the system to other conventional Fe and Ru-based catalysts can be achieved; that is, the synergy between LiH and Fe may lie in the formation of the active center composed of Li–Fe ternary hydrides that are capable of activating and hydrogenating $N_2$ in an energetically more favorable manner, forming [Fe-$NH_2$-Li] and $LiNH_2$-containing intermediates that can be further hydrogenated to $NH_3$ at lower temperatures. The relocation of N to Li will enable the occurrence of a final hydrogenation step at $LiNH_2$ (that is, $LiNH_2 + H_2 \rightarrow LiH + NH_3$) rather than on Fe; therefore, the TM exerted scaling relation will be intervened. In contrast, ammonia formation on conventional TM-based catalysts is carried out on some active sites composed of multiple TM atoms (for example, the C7 site for Fe and B5 site for Ru)[3a,b,14] where $N_2$ undergoes homolytic cleavage and subsequent hydrogenation, which are distinctly different from the occurrences in the Fe-LiH catalytic system.

A step further from the present observations, and perhaps more intriguing, concerns whether, and how, H in the Li–Fe hydrides participates in the activation of $N_2$, a subject related to a decades-long debate. It is generally believed that $N_2$ activation in biochemical and homogeneous $N_2$ fixation occurs by an H-associated mechanism, and experimental evidence supports this proposal.[2b–d,15] In the heterogeneous catalysis domain, the majority of experimental and theoretical results, on the other hand, favor dissociative activation because of the concerted efforts of multiple TMs and the strong bonding of N to metal surfaces. The lack of proxy Fe atoms in the Li–Fe ternary hydride active center, however, infers that the activation of N≡N may go through a distal or alternative hydrogenation manner that could resemble the mechanism proposed in biochemical and homogeneous N fixation;[2b–d] although more concrete and supportive evidence needs to be acquired. Hydrogen atoms in Li-Fe-H species bear more electrons and are thus highly reductive. Therefore, interaction of Li-Fe-H with chemisorbed $N_2$ would exhibit unique behavior compared to that of protons in homogeneous $N_2$ fixation and the chemisorbed H in the conventional heterogeneous catalysis on Fe or Ru surfaces. The electron shuffling from hydridic H to $N_2$ has to be mediated, very likely by Fe, a topic that is worthy of in-depth experimental and theoretical investigations. Although a conclusive statement on this aspect cannot be drawn at this moment, the present investigation discusses, for the first time, the importance of Li–Fe ternary hydrides in ammonia synthesis. We believe that with further experimental and theoretical effort, better understanding can be achieved that will benefit catalyst design and development for energy-efficient ammonia synthesis. Such advances may be integrated into clean and renewable energy-harvesting and -storage technology.

## Acknowledgements

The authors would like to acknowledge financial support from the projects National Natural Science Funds for Distinguished Young Scholars (51225206), National Natural Science Foundation of China (21327901, 21503222, 21603220, 21633011, and 21673231), Dalian Institute of Chemical Physics (DICP DMTO201504), the Collaborative Innovation Center of Chemistry for Energy Materials (2011-iChEM), and the State Key Laboratory of Physical Chemistry of Solid Surfaces, Xiamen University (201504).

## Conflict of interest

The authors declare no conflict of interest.

**Keywords:** ammonia synthesis · clusters · iron catalysts · $Li_4FeH_6$ · optical spectroscopy

**How to cite:** *Angew. Chem. Int. Ed.* **2017**, *56*, 8716–8720
*Angew. Chem.* **2017**, *129*, 8842–8846

[1] a) J. W. Erisman, M. A. Sutton, J. Galloway, Z. Klimont, W. Winiwarter, *Nat. Geosci.* **2008**, *1*, 636–639; b) R. Schlögl, *Angew. Chem. Int. Ed.* **2003**, *42*, 2004–2008; *Angew. Chem.* **2003**, *115*, 2050–2055; c) C. Zamfirescu, I. Dincer, *J. Power Sources* **2008**, *185*, 459–465.

[2] a) T. H. Rod, A. Logadottir, J. K. Norskov, *J. Chem. Phys.* **2000**, *112*, 5343–5347; b) D. V. Yandulov, R. R. Schrock, *Science* **2003**, *301*, 76–78; c) K. Arashiba, Y. Miyake, Y. Nishibayashi, *Nat. Chem.* **2011**, *3*, 120–125; d) J. S. Anderson, J. Rittle, J. C. Peters, *Nature* **2013**, *501*, 84–87; e) A. Vojvodic, A. J. Medford, F. Studt, F. Abild-Pedersen, T. S. Khan, T. Bligaard, J. K. Norskov, *Chem. Phys. Lett.* **2014**, *598*, 108–112.

[3] a) D. R. Strongin, J. Carrazza, S. R. Bare, G. A. Somorjai, *J. Catal.* **1987**, *103*, 213–215; b) R. C. Egeberg, S. Dahl, A. Logadottir, J. H. Larsen, J. K. Nørskov, I. Chorkendorff, *Surf. Sci.* **2001**, *491*, 183–194; c) J. J. Mortensen, M. V. Ganduglia-Pirovano, L. B. Hansen, B. Hammer, P. Stoltze, J. K. Norskov, *Surf. Sci.* **1999**, *422*, 8–16.

[4] a) K. Aika, A. Ozaki, H. Hori, *J. Catal.* **1972**, *27*, 424–431; b) G. Ertl, M. Weiss, S. B. Lee, *Chem. Phys. Lett.* **1979**, *60*, 391–394; c) S. Dahl, A. Logadottir, C. J. H. Jacobsen, J. K. Norskov, *Appl. Catal. A* **2001**, *222*, 19–29; d) W. J. B. J. G. van Ommen, J. Prasad, P. Mars, *J. Catal.* **1975**, *38*, 120–127; e) S. R. Bare, D. R. Strongin, G. A. Somorjai, *J. Phys. Chem.* **1986**, *90*, 4726–4729.

[5] F. Abild-Pedersen, J. Greeley, F. Studt, J. Rossmeisl, T. R. Munter, P. G. Moses, E. Skulason, T. Bligaard, J. K. Norskov, *Phys. Rev. Lett.* **2007**, *99*, 016105.

[6] P. Wang, F. Chang, W. Gao, J. Guo, G. Wu, T. He, P. Chen, *Nat. Chem.* **2017**, *9*, 64–70.

[7] a) A. W. Castleman, R. G. Keesee, *Acc. Chem. Res.* **1986**, *19*, 413–419; b) H. J. Freund, G. Meijer, M. Scheffler, R. Schlogl, M.

  

Wolf, *Angew. Chem. Int. Ed.* **2011**, *50*, 10064 – 10094; *Angew. Chem.* **2011**, *123*, 10242 – 10275.
[8] a) D. K. Böhme, H. Schwarz, *Angew. Chem. Int. Ed.* **2005**, *44*, 2336 – 2354; *Angew. Chem.* **2005**, *117*, 2388 – 2406; b) X.-L. Ding, X.-N. Wu, Y.-X. Zhao, S.-G. He, *Acc. Chem. Res.* **2012**, *45*, 382 – 390; c) N. Dietl, T. Wende, K. Chen, L. Jiang, M. Schlangen, X. Zhang, K. R. Asmis, H. Schwarz, *J. Am. Chem. Soc.* **2013**, *135*, 3711 – 3721; d) Z. Luo, A. W. Castleman, Jr., S. N. Khanna, *Chem. Rev.* **2016**, *116*, 14456 – 14492.
[9] A. Borodziński, M. Bonarowska, *Langmuir* **1997**, *13*, 5613 – 5620.
[10] F. Rosowski, A. Hornung, O. Hinrichsen, D. Herein, M. Muhler, G. Ertl, *Appl. Catal. A* **1997**, *151*, 443 – 460.
[11] a) T. K. Firman, C. R. Landis, *J. Am. Chem. Soc.* **1998**, *120*, 12650 – 12656; b) W. Bronger, T. Sommer, G. Auffermann, P. Müller, *J. Alloys Compd.* **2002**, *330 – 332*, 536 – 542; c) T. Sato, S. Takagi, M. Matsuo, K. Aoki, S. Deledda, B. C. Hauback, S. Orimo, *Mater. Trans.* **2014**, *55*, 1117 – 1121.
[12] H. Saitoh, S. Takagi, M. Matsuo, Y. Iijima, N. Endo, K. Aoki, S. Orimo, *APL Mater.* **2014**, *2*, 076103.
[13] D. A. Hall, G. J. Leigh, *J. Chem. Soc. Dalton* **1996**, 3539 – 3541.
[14] S. Dahl, A. Logadottir, R. C. Egeberg, J. H. Larsen, I. Chorkendorff, E. Törnqvist, J. K. Nørskov, *Phys. Rev. Lett.* **1999**, *83*, 1814 – 1817.
[15] a) F. Studt, F. Tuczek, *Angew. Chem. Int. Ed.* **2005**, *44*, 5639 – 5642; *Angew. Chem.* **2005**, *117*, 5783 – 5787; b) F. Neese, *Angew. Chem. Int. Ed.* **2006**, *45*, 196 – 199; *Angew. Chem.* **2006**, *118*, 202 – 205.

Manuscript received: April 10, 2017
Accepted manuscript online: May 29, 2017
Version of record online: June 12, 2017

  